

Effects of post-Newtonian Spin Alignment on the Distribution of Black-Hole Recoils

Emanuele Berti,^{1,2,*} Michael Kesden,^{3,†} and Ulrich Sperhake^{4,1,2,5,‡}

¹*Department of Physics and Astronomy, The University of Mississippi, University, MS 38677, USA*

²*California Institute of Technology, Pasadena, CA 91109, USA*

³*Center for Cosmology and Particle Physics, New York University, 4 Washington Pl., New York, NY 10003, USA*

⁴*Institut de Ciències de l'Espai (CSIC-IEEC), Facultat de Ciències, Campus UAB, E-08193 Bellaterra, Spain*

⁵*Centro Multidisciplinar de Astrofísica – CENTRA, Departamento de Física,*

Instituto Superior Técnico – IST, 1049-001 Lisboa, Portugal

(Dated: April 21, 2019)

Recent numerical relativity simulations have shown that the final black hole produced in a binary merger can recoil with a velocity as large as 5,000 km/s. Because of enhanced gravitational-wave emission in the so-called “hang-up” configurations, this maximum recoil occurs when the black-hole spins are partially aligned with the orbital angular momentum. We revisit our previous statistical analysis of post-Newtonian evolutions of black-hole binaries in the light of these new findings. We demonstrate that despite these new configurations with enhanced recoil velocities, spin alignment during the post-Newtonian stage of the inspiral will still significantly suppress (or enhance) kick magnitudes when the initial spin of the more massive black hole is more (or less) closely aligned with the orbital angular momentum than that of the smaller hole. We present a preliminary study of how this post-Newtonian spin alignment affects the ejection probabilities of supermassive black holes from their host galaxies with astrophysically motivated mass ratio and initial spin distributions. We find that spin alignment suppresses (enhances) ejection probabilities by $\sim 40\%$ (20%) for an observationally motivated mass-dependent galactic escape velocity, and by an even greater amount for a constant escape velocity of 1,000 km/s. Kick suppression is thus at least a factor two more efficient than enhancement.

PACS numbers: 04.25.dg, 04.70.Bw, 04.30.-w

I. INTRODUCTION

Supermassive black holes (SBHs) reside at the centers of most large galaxies. The masses of these SBHs are tightly correlated with the luminosity [1], mass [2], and velocity dispersions [3] of the spheroidal components of their host galaxies. Large galaxies form hierarchically from the merger of smaller galaxies, and SBH mergers are expected to accompany the mergers of their hosts. The final stages of these SBH mergers are driven by the emission of copious amounts of gravitational radiation. Conservation of linear momentum implies that the final black holes produced in SBH mergers must recoil with linear momentum equal in magnitude and opposite in direction to that of the anisotropically emitted gravitational radiation. Early estimates of these gravitational recoils or “kicks” using post-Newtonian (PN) techniques [4] and black-hole perturbation theory [5] suggested that they would not exceed several hundred km/s in magnitude. More recently, progress in numerical relativity (NR) [6–8] has allowed relativists to simulate the mergers of highly spinning, comparable-mass black holes. For non-spinning binaries, ensuing studies identified a maximum recoil of 175 km/s [9]. Simulations of spinning black holes, however, resulted in one of the greatest surprises

of numerical relativity; for equal-mass binaries with opposite spins in the orbital plane gravitational recoils can approach 4,000 km/s [10, 11], greater than the escape velocity of even the most massive galaxies. This theoretical result seems at first difficult to reconcile with observations indicating that almost all large galaxies host SBHs.

One solution to this problem is to align the SBH spins before merger into configurations that lead to small recoils. Gravitational radiation extracts energy and angular momentum from the orbit of the binary SBHs, causing them to merge on a timescale $t_{\text{GR}} \propto r^4$, where r is the binary separation. This timescale becomes longer than the age of the universe at separations $r \sim 1$ pc, implying that some mechanism other than gravitational radiation is required to escort the SBHs to this separation (the “final-parsec problem”) [12]. One such mechanism is the transfer of orbital angular momentum from the SBH binary to surrounding gas. This gas forms a circumbinary disk about the SBHs, but can still be transferred through the gap onto accretion disks about the individual SBHs [13]. If the angular momentum of the circumbinary disk is misaligned with the SBH spins, the Lense-Thirring effect causes inclined annuli in the individual accretion disks to differentially precess about the SBH spins. Bardeen and Petterson [14] showed that viscous dissipation causes this differentially precessing gas to settle into the equatorial planes of the SBHs. On longer timescales, these warped accretion disks torque the SBH spins into alignment with the orbital angular momentum of the gas at large radii, presumably that of the circumbinary disk from which

* berti@phy.olemiss.edu

† mhk10@nyu.edu

‡ sperhake@tapir.caltech.edu

both accretion disks are being fed [15]. Bogdanović et al. [16] suggested that this alignment could reduce gravitational recoils to less than 200 km/s, in contrast to the $\sim 4,000$ km/s recoils expected for SBHs in the “superkick” configuration (spins in opposite directions lying in the equatorial plane) [10, 11].

Dotti et al. [17] tested this suggestion by performing a series of N-body smoothed particle hydrodynamics (SPH) simulations of two $4 \times 10^6 M_\odot$ SBHs inspiraling due to dynamical friction exerted by a $10^8 M_\odot$ circumnuclear disk in their orbital plane. One of the SBHs began at the center of the circumnuclear disk, while the second SBH spiraled inwards from an initial separation of 50 pc to a final separation of ~ 10 pc. Gas particles within the Bondi-Hoyle radii [18] of the SBHs were accreted, and assumed to fuel warped accretion disks as described in Perego et al. [15]. On a timescale of $\lesssim 1\text{-}2$ Myr, the SBH spins became aligned to within 10° (30°) of their orbital angular momentum for a cold (hot) circumnuclear disk [19]. If the partially aligned spin configurations found in these simulations were preserved as the SBHs inspiraled and merged, the median recoils predicted by NR simulations would be $\lesssim 100$ km/s for dimensionless spins χ_i ($i = 1, 2$) with an initially uniform distribution of magnitudes $\chi_i \in [0, 1]$.

The assumption that SBH spin distributions remain unchanged between $r \simeq 10$ pc $\simeq 10^8 R_S$ ($M_{\text{BH}}/10^6 M_\odot$) $^{-1}$ (where the SPH simulations end) and $r \simeq 5 R_S$ (where the NR simulations begin), needs further examination. Here $R_S = 2GM_{\text{BH}}/c^2$ is the Schwarzschild radius of a SBH of mass M_{BH} . Because of the steep scaling $t_{\text{GR}} \propto r^4$ mentioned previously, the SBHs decouple from their circumbinary disk and spiral inwards purely under the influence of gravitational radiation at a binary separation $r_{\text{dec}} \simeq 10^2 - 10^3 M$ [12], where $M = m_1 + m_2$ is the total mass of the binary. Schnittman [20] integrated PN equations of motion and spin precession from an initial binary separation $r_i = 1000M$ to a final separation $r_f = 10M$ (in geometrical units where $G = c = 1$) and discovered that partially aligned SBH spin distributions during this portion of the inspiral are strongly influenced by the presence of spin-orbit resonances.

These resonances are special spin configurations in which both SBH spins and the orbital angular momentum jointly precess at the same frequency in a common two-dimensional plane. For binary SBHs with mass ratio $q \equiv m_2/m_1 \leq 1$ and dimensionless spins χ_i , at each separation r there exist two one-parameter families of spin-orbit resonances: one with $\Delta\phi = 0^\circ$ and the other with $\Delta\phi = 180^\circ$, where $\Delta\phi$ is the angle between the components of χ_1 and χ_2 perpendicular to the orbital angular momentum \mathbf{L} . The first of these families ($\Delta\phi = 0^\circ$) has $\theta_1 < \theta_2$, where $\theta_i \equiv \arccos(\chi_i \cdot \hat{\mathbf{L}})$, while the second family ($\Delta\phi = 180^\circ$) has $\theta_1 > \theta_2$. As SBHs inspiral due to the emission of gravitational radiation, they can become captured into nearby spin-orbit resonances, substantially altering the SBH spin distributions between r_i and r_f .

In previous work, we examined the influence of this PN portion of the inspiral on the expected distribution of SBH final spins [21] and recoils [22]. We found that if the spin of the more massive SBH was more closely aligned with the orbital angular momentum ($\theta_1 < \theta_2$), the SBHs were more likely to be captured into the $\Delta\phi = 0^\circ$ family of resonances. This alignment of the SBH spins prior to merger causes them to add constructively, enhancing the spin of the final black hole. Symmetry requirements imply that gravitational recoils are suppressed when the SBH spins are aligned with each other prior to merger [23, 24], so this PN alignment also reduces the predicted distribution of recoils. The opposite is true when $\theta_1 > \theta_2$; SBHs are preferentially captured into the $\Delta\phi = 180^\circ$ family of resonances, reducing the final spins and enhancing the gravitational recoils.

Recent equal-mass NR simulations by Lousto and Zlochower ([25, 26]; henceforth LZ) have qualitatively and quantitatively changed the predicted dependence of gravitational recoils on the SBH spins χ_i . The maximum possible kick, extrapolated to maximal initial spins, is now $\sim 4,900$ km/s, and this kick occurs not in the previously described “superkick” configuration but for spins with $\theta_i \simeq 50^\circ$. In light of these new findings, it is worth investigating whether PN spin alignment still has as dramatic an effect on the expected recoil distribution as we found previously. This investigation is the subject of this paper. In Section II we revisit our analysis of how PN evolution affects binaries that are evolved from an initial separation of $r_i = 1000M$ down to a final separation of $r_f = 10M$. We clarify the reason why spin-orbit resonances are also effective at suppressing kicks consistent with the new LZ results. In Section III we set up a more extensive set of Monte Carlo simulations of SBH inspirals. We focus on a specific choice for the initial distribution of SBH parameters $\{q, \chi_1, \chi_2\}$, and justify this choice based on astrophysical considerations. In Section IV we present the final distributions of recoil velocities resulting from our Monte Carlo simulations, and our predictions for the fraction of remnant SBHs that are ejected from their host galaxies. We summarize these results and discuss the sources of uncertainty in our analysis in Section V.

II. POST-NEWTONIAN SPIN ALIGNMENT

The recent LZ simulations [25, 26] have two potentially important consequences from an astrophysical point of view. First of all, the maximum possible “hang-up” kick magnitude is about 25% larger than predicted by the ordinary, “no hang-up” superkick formula: 4,900 km/s rather than 3,750 km/s. Secondly, the largest kick occurs for a configuration in which the spins are partially aligned with the orbital angular momentum. Because of the gas-dynamical alignment arguments summarized above, this configuration seems more likely than the superkick configuration. We would therefore expect an enhancement in the statistical likelihood of gravitational recoils eject-

ing remnant SBHs from galaxies as reported by LZ. We confirm this enhancement, but show that even in hang-up kick scenarios spin-orbit resonances can significantly change the likelihood of large recoil velocities as the SBHs inspiral from sub-parsec scales to about $10M$.

The largest “superkick” recoil velocities are obtained for nearly equal-mass SBHs. Furthermore, the LZ kick formula is most reliable for mass ratios close to unity, since all 48 of the new NR simulations were carried out for $q = 1$ [26]. We therefore begin our study of the likelihood of very large kicks by considering comparable-mass binaries. Resonance effects are not present for $q = 1$, but astrophysical binaries are not expected to be precisely equal in mass. For this reason we have performed Monte Carlo PN evolutions of 900 black hole binaries with mass ratio close to but not exactly equal to one (we choose $q = 9/11$ to facilitate comparisons with Schnittman [20] and our own earlier work [21, 22]). We considered binaries where the two black holes have the same dimensionless spin magnitude $\chi_1 = \chi_2 = \chi$, and selected five equally-spaced values of χ in the range $[0.5, 1.0]$. For each of the five values of χ we further selected six equally-spaced initial values of θ_1 in the range $[5^\circ, 30^\circ]$, for a total of thirty Monte Carlo simulations. Each simulation is started by assuming uniform distributions in $\Delta\phi \in [0, 2\pi]$ and $\cos\theta_2 \in [-1, 1]$. We begin at an initial separation $r_i = 1000M$ and use the PN equations of motion to evolve the binaries down to a final separation $r_f = 10M$ (cf. Section II of [21] for details of the PN evolution).

To quantify the effect of PN spin alignment, we compute the recoil velocity distribution that would result from applying kick formulae to our binaries *before* the PN evolution (at $r_i = 1000M$) and close to merger (at $r_f = 10M$). We calculate the component v_{\parallel} of the recoil velocity parallel to \mathbf{L} using both the new LZ “hang-up” formula [25, 26] and the older kick formula from Campanelli et al. [11]. We calculate the components v_m , v_{\perp} perpendicular to \mathbf{L} from the fitting formula of [11]: cf. Eq. (1) in [22]. We then compute the probability that the total recoil velocity is greater than $v_{\text{ej}} = 1,000$ km/s for each of our thirty Monte Carlo simulations (six values of θ_1 and five values of χ). This value of v_{ej} is comparable to the escape velocity from a giant elliptical galaxy [27]; we will consider more realistic escape velocities that depend on the host galaxy’s mass in Section IV. The results are plotted in Figure 1.

Figure 1 confirms LZ’s conclusion that the “hang-up” effect increases ejection probabilities. By comparing the dashed lines in the left and right panels of Figure 1, we see that, if we ignore the effect of resonances (as the authors of the LZ papers did), ejection probabilities are only mildly dependent on θ_1 and roughly double because of the hang-up kick effect. These ejection probabilities can be larger than 50% for spins $\chi \gtrsim 0.8$ and $q = 9/11$. On the other hand, a comparison of dashed and solid lines in each panel shows that ejection probabilities are dramatically reduced if we apply the kick formula (as we

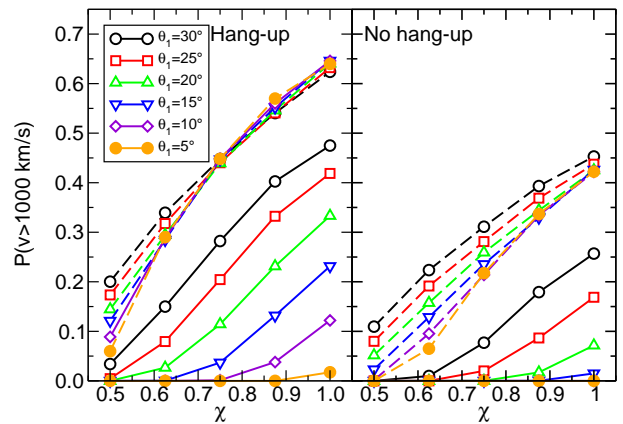


FIG. 1. Probability of having a recoil velocity $v > 1,000$ km/s as a function of dimensionless spin magnitude $\chi_1 = \chi_2 = \chi$ for binaries with mass ratio $q = 9/11$. The initial value of θ_1 is indicated by the different symbols, while the spin χ_2 of the smaller SBH is initially isotropically distributed. Left panel: prediction according to the LZ papers [25, 26]; right panel: prediction without this newly discovered hang-up effect. In all plots the dashed lines correspond to the initial distributions at $r_i = 1000M$, while the solid lines give the distributions at $r_f = 10M$, after PN spin alignment has occurred.

should) close to merger, rather than at large separations. The relevance of resonant effects depends on θ_1 : if the initial angle between the larger black hole and the orbital angular momentum $\theta_1 < 10^\circ$, recoil velocities larger than $v_{\text{ej}} \sim 1,000$ km/s would almost never occur. Even for more modest alignments ($\theta_1 < 30^\circ$), such large kicks only occur for large values of χ . Recoils are even smaller for $q < 9/11$, as all components of the kick are proportional to $q^2/(1+q)^5$ (see Eq. (11) of [26]). Note that this kick suppression only applies when on average $\theta_1 < \theta_2$; for initial values of $\theta_1 > \theta_2$ the recoil would be enhanced, not suppressed.

It may seem surprising that PN spin alignment so dramatically suppresses the recoil velocities predicted by the new LZ kick formula, since many of the spin-orbit resonances depicted in Figure 1 of [21] have values of θ_i comparable to that of the new “maximum recoil” configuration in the presence of the hang-up effect. We can understand the effectiveness of PN kick suppression by recognizing that it results from the alignment of the perpendicular components of the SBH spins *with each other* ($\Delta\phi \rightarrow 0^\circ$), not from the spins aligning with the orbital angular momentum ($\theta_i \rightarrow 0$, as Bogdanović et al. [16] argued would occur due to the torque exerted by a warped circumbinary disk).

To illustrate this point, we consider maximally spinning ($\chi_1 = \chi_2 = 1$) binaries with $q = 9/11$ in Figure 2. Dotted histograms refer to recoil distributions computed before the PN evolutions (at $r_i = 1000M$), and solid histograms refer to the corresponding distributions computed after evolving the binaries down to $r_f = 10M$.

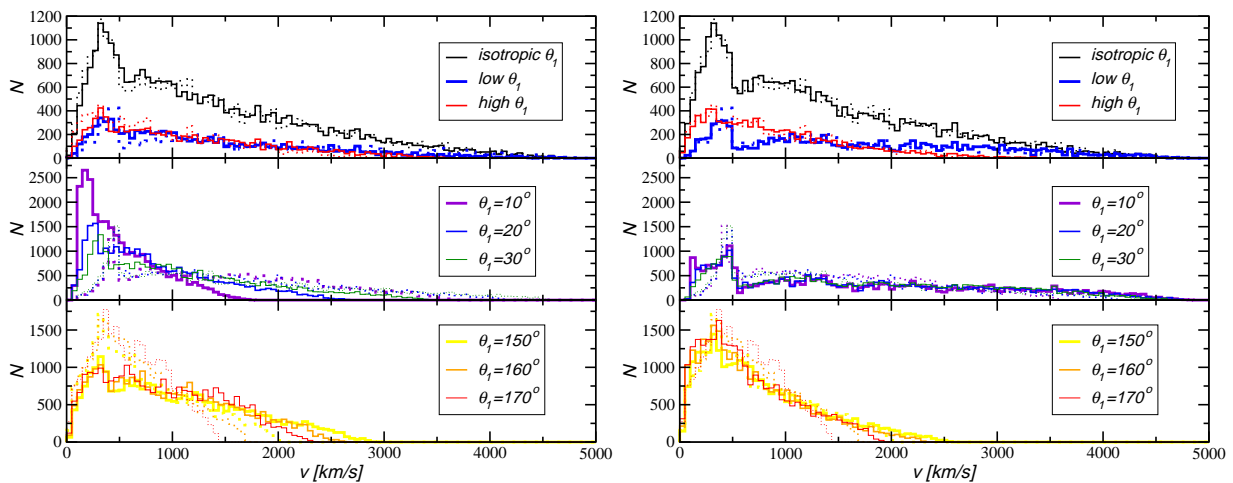


FIG. 2. Left panel: histograms of the recoil velocity v for maximally spinning ($|\chi_i| = 1$) BH mergers with mass ratio $q = 9/11$. Dotted lines show the recoils expected if the BHs merge with the parameters specified at initial separation $r_i = 1000M$. Solid curves show the expected kicks if the BHs precess as described in Section 2 of [22] from r_i to $r_f = 10M$ prior to merger. Right panel: same as in the left panel, except that here the solid histograms show the velocity distribution obtained when $\Delta\phi$ is reset to a flat distribution $\Delta\phi \in [0, 180^\circ]$ after the binaries reach r_f .

Let us first focus on the left panel. The black curves in the upper histogram show that black holes with isotropic spin distributions (flat distributions in $\cos\theta_1$, $\cos\theta_2$, and $\Delta\phi$) maintain these isotropic distributions as they inspiral down to $r_f = 10M$. The thick blue (thin red) curves in the upper histogram corresponds to the subset of this isotropic distribution with the 30% lowest (highest) initial values of θ_1 . Careful comparison of the solid and dotted curves reveals that recoils are suppressed (enhanced) for low (high) initial values of θ_1 . This tendency is seen much more clearly in the middle and lower panels, where θ_1 has the indicated initial value while χ_2 retains its isotropic initial distribution. If \mathbf{S}_1 is partially aligned with \mathbf{L} , as in the middle histograms, then θ_{12} (the angle between the two spins) and $\Delta\phi$ will be strongly peaked around 0° at the end of the evolution and kicks will be reduced. If instead \mathbf{S}_1 is partially anti-aligned with \mathbf{L} (as in the lower histograms), then θ_{12} and $\Delta\phi$ will be strongly peaked around 180° at the end of the evolution and the kicks will be enhanced (cf. the discussion in [22]). The crucial element for producing alignment here is the fact that $\Delta\phi \rightarrow 0^\circ$. This is illustrated in the right-hand panels of Figure 2, which are the same as the corresponding left-hand panels, except that $\Delta\phi$ has been reset to a flat distribution $\Delta\phi \in [0, 180^\circ]$ after the PN inspiral (but before the recoil velocities are computed). This nearly eliminates the kick suppression (for initially aligned binaries) or enhancement (for initially anti-aligned binaries).

III. ASTROPHYSICAL PARAMETERS

We demonstrated in the previous section that the new fitting formulae for gravitational recoils provided in the

LZ papers [25, 26] did not alter our earlier conclusion [22] that PN spin alignment can dramatically affect the distribution of recoil velocities for specific initial values of q and θ_1 and an initially isotropic distribution for χ_2 . In this section, we describe a more astrophysically motivated choice for these initial parameters. The effect of PN spin alignment on this new distribution will be presented in Section IV.

A. Mass Ratio

The origin of SBHs is poorly understood theoretically and poorly constrained observationally. Lynden-Bell [28] recognized that the central objects of mass $10^7 - 10^9 M_\odot$ believed to power quasars would quickly collapse into SBHs. Haehnelt and Rees [29] explained the quasar luminosity function by assuming that such massive SBH seeds promptly formed at the centers of dark-matter (DM) halos whose formation rates could be predicted using the Press-Schechter formalism [30]. More recent theoretical work has called into question whether the high-redshift seeds of SBHs were truly this massive. While some maintain that massive central concentrations of gas at the centers of pre-galactic disks can directly collapse into $\sim 10^5 M_\odot$ SBH seeds [31], others argue that metal-free gas will fragment into Population III stars with characteristic masses $\gtrsim 100 M_\odot$ [32]. Volonteri, Haardt, and Madau [33], also using the Press-Schechter formalism to estimate halo mass functions and merger rates, showed that $150 M_\odot$ seeds occupying $3.5 - 4\sigma$ overdensities at redshift $z = 20$ could grow into SBHs that would reproduce both the quasar luminosity function at $1 \leq z \leq 5$ and the observed local $M_{\text{BH}} - \sigma$ relation [3] between

SBH mass and galaxy velocity dispersion. The European New Gravitational Wave Observatory (NGO), also informally known as “eLISA”, will be able to distinguish between these two different scenarios for SBH formation by observing the gravitational waves emitted during high-redshift mergers [34–37].

Given this uncertainty in the high-redshift population of SBH seeds, in this paper we restrict our attention to SBH mergers in the low-redshift ($z \lesssim 1$) universe. Stewart et al. [38] used a high-resolution N-body simulation to calculate the merger rates of DM halos in the redshift range $0 \leq z \leq 4$. They fit their results for the rate at which a larger galaxy of mass M_g merges with smaller galaxies with masses between m_g and M_g to the function

$$\frac{dN_{\text{merg}}}{dt}(M_g, m_g) = A_t(M_g)F(m_g/M_g), \quad (1)$$

where the normalization $A_t(M_g)$ is binned by mass, and the mass-ratio dependence is given by

$$F(m_g/M_g) = \left(\frac{m_g}{M_g}\right)^{-c} \left(1 - \frac{m_g}{M_g}\right)^d, \quad (2)$$

with the indices c and d determined from the simulation. This same functional form can be used for the merger rates of both DM halos of mass M_h and galaxies with stellar mass M_* , although the fitted values of the parameters will be different. Table 1 of Stewart et al. [38] provides numerical estimates of these parameters binned by stellar mass; we use the functions

$$A_t(M_*) = 0.0098 \text{ Gyr}^{-1} \left(\frac{M_*}{10^{10} M_\odot}\right)^{0.736}, \quad (3a)$$

$$c = 0.329 \left(\frac{M_*}{10^{10} M_\odot}\right)^{-0.158}, \quad (3b)$$

$$d = 1.1 - 0.2z, \quad (3c)$$

which approximate the values listed in this table. Note that the total rate of mergers diverges in the limit $m_g \rightarrow 0$ for $c > 0$, although the rate at which the galactic mass increases remains finite. The Press-Schechter formalism also predicts that the number of DM halos and thus the number of mergers diverges as their mass goes to zero. Volonteri, Haardt, and Madau [33] address this issue in their merger trees by only keeping track of halos with masses above an effective mass resolution M_{res} that evolves with redshift, but always remains a small fraction of the largest progenitor mass. Because we are only interested in SBH mergers at low redshift, we neglect galaxies with $M_* < 10^9 M_\odot$. This corresponds to neglecting SBHs with $m_i < 10^6 M_\odot$, since SBHs are about a fraction of 10^{-3} of the stellar mass of their host spheroids [39]. SBHs less massive than this value are poorly constrained observationally, and even if present in a halo may have difficulty reaching the galactic center, since the dynamical friction time scales as the inverse of the SBH mass. We assume that SBH mergers occur promptly following the merger of their host galaxies.

Eq. (1) gives the rate at which individual galaxies of stellar mass M_* merge with smaller galaxies; to determine the total rate of mergers in a cosmological volume also requires an estimate of the galactic stellar mass function $dN_g/d\log M_*$. We use the mass function determined from the $z \sim 0.37$ sample of the COSMOS survey [40]; this mass function, as shown in the left panel of Figure 14 of [40], is quite similar to earlier mass functions derived from the Sloan Digital Sky Survey [41–43]. The total rate per unit cosmological volume $R(M_*)$ at which galaxies with stellar masses between $10^9 M_\odot$ and M_* merge is given by

$$R(M_*) = \int_9^{\log M_*} \frac{dN_g}{d\log M_*} \frac{dN_{\text{merg}}}{dt}(M', 10^9 M_\odot) d\log M'. \quad (4)$$

We use this rate function as part of a Monte Carlo approach to generate a representative sample of SBH mergers. We choose a random number r_1 from a flat distribution in the interval $0 \leq r_1 \leq 1$, then find the stellar mass M_* for which $R(M_*) = r_1 R(\infty)$. Values of $r_1 \simeq 0$ correspond to stellar masses $M_* \simeq 10^9 M_\odot$, while values $r_1 \simeq 1$ correspond to stellar masses $M_* \simeq 10^{12} M_\odot$ above which the galactic luminosity function is exponentially suppressed. We next choose a second random number r_2 , also from a flat distribution $0 \leq r_2 \leq 1$, and find the value of m_* for which $F(m_*/M_*) = r_2 F(10^9 M_\odot/M_*)$. Values of $r_2 \simeq 0$ correspond to nearly equal-mass mergers ($m_* \lesssim M_*$), while values $r_2 \simeq 1$ correspond to mergers with the smallest galaxies to host SBHs ($m_* \simeq 10^9 M_\odot$). The SBH masses are then determined from the masses of their host galaxies, $m_1 = 10^{-3} M_*$ and $m_2 = 10^{-3} m_*$.

This procedure for determining the SBH mass ratio $q = m_2/m_1$ is considerably more elaborate than that used in the LZ papers [25, 26]. They assumed that the probability of having a SBH mass ratio between q and $q + dq$ was simply $F(q)dq$, with the function $F(q)$ given by Eq. (2) with $c = 0.3$ and $d = 1$. This assumption seems to be based on a misinterpretation of Stewart et al. [38], which defines $F(q)$ as being proportional to the total number of mergers between a mass ratio of q and 1. The LZ papers did not need to introduce an explicit cutoff at small mass ratios, because the total number of mergers remained finite under their assumption. This finite number of mergers allowed them to calculate the probability that the gravitational recoil would be in a particular velocity interval. Given the infinite rate of mergers predicted by Eq. (1) as $m_* \rightarrow 0$, we would predict an infinite number of mergers with $v = 0$ km/s in the absence of a cutoff, since $v \propto q^2$ as $q \rightarrow 0$. This cutoff is well justified physically because DM halos of arbitrarily small mass cannot host stars, let alone SBHs.

B. Initial Spins

The accretion and merger history of SBHs determines the magnitude and direction of their spins.

1. Spin Magnitudes

Volonteri et al. [44] examined the distribution of SBH spin magnitudes using cosmological merger trees constructed within the Press-Schechter formalism. They found that binary mergers alone lead to broad distributions of the dimensionless spin magnitude peaked around $\chi \simeq 0.5$, but that when accretion is included the spins reach much larger values. Accretion from geometrically thin disks [45] leads to spin distributions sharply peaked around $\chi \simeq 0.998$ [46], as the Bardeen-Petterson effect [14] aligns the SBH spins with the disks on a timescale [15]

$$t_{\text{al}} \sim 10^5 \chi^{5/7} \left(\frac{M}{10^6 M_\odot} \right)^{-2/35} \left(\frac{f_{\text{Edd}}}{\eta_{0.1}} \right)^{-32/35} \text{ yr}, \quad (5)$$

much shorter than the Salpeter time

$$t_{\text{Edd}} \simeq 4.6 \times 10^7 \left(\frac{\eta_{0.1}}{f_{\text{Edd}}} \right) \text{ yr} \quad (6)$$

on which the spin magnitudes change. Here $\eta_{0.1}$ is the radiative efficiency normalized by a typical value 0.1 and f_{Edd} is the AGN luminosity in units of the Eddington value $L_{\text{Edd}} = 4\pi GM_{\text{BH}} c m_p / \sigma_T$ (m_p is the proton mass, σ_T is the Thomson cross section for elastic scattering). Accretion from geometrically thick disks leads to much broader spin distributions, because spin alignment occurs on the longer Salpeter time. SBHs that accrete from a thick disk may also have a smaller maximum spin $\chi \simeq 0.93$, as ordered magnetic fields in the plunging region interior to the innermost stable orbit may extract angular momentum that would be advected by the SBH in the thin-disk case [47].

Volonteri et al. [44] assumed that after each major merger, SBHs accreted continuously from disks with well defined angular momentum until their mass increased by an amount $\Delta m = 3.6 \times 10^6 V_{c,150}^{5.2} M_\odot$, where $V_{c,150}$ is the circular velocity of the host galaxy's DM halo in units of 150 km/s. Moderski and Sikora [48] proposed an alternative scenario, in which gas was accreted in small discrete episodes with random orientations with respect to the SBH spin. This ‘‘chaotic accretion’’ scenario leads to SBH spins that fluctuate about $\chi = 0$, and was originally motivated by the conjecture of Wilson and Colbert [49] that only 10% of AGN that are radio-loud are powered by highly spinning SBHs. King et al. [50] suggested that the mass accreted in each of these discrete episodes might be determined by the mass of the accretion disk interior to the radius $r_{\text{sg}} \sim 0.01 - 0.1$ pc at which the disk becomes self-gravitating. Star formation at $r > r_{\text{sg}}$ would stir the gas flow, implying that each event would have essentially random orientations. Recent high-resolution N-body/SPH simulations of galactic accretion disks which include star formation support this suggestion [51]. These simulations follow gas flows from galactic scales of ~ 100 kpc all the way down to < 0.1 pc, and show that the orientation of the inner nuclear disk

varies on \sim Myr timescales, that are comparable to the alignment timescale t_{al} of Eq. (5).

Berti and Volonteri [52] explored how chaotic accretion would affect SBH spin evolution in a cosmological context, also incorporating the results of NR simulations available at the time. The NR simulations implied that SBH spin distributions would now be broadly peaked about $\chi \sim 0.7$ in the absence of accretion, but that the full range of spin magnitudes $0 \leq \chi \leq 1$ was now possible once both standard and chaotic accretion were permitted. This differs from the spin magnitude distributions used in the LZ papers [25, 26], which as shown in Figure 7 of [26] are peaked around $\chi \simeq 0.8$. These spin distributions were determined from the N-body/SPH simulations of Dotti et al. [19], which were restricted to equal-mass binaries, and began with an initially uniform distribution of spin magnitudes $\chi_i \in [0, 1]$. Although the $\lesssim 10$ Myr duration of these simulations is long compared to the alignment time t_{al} on which the spin directions change, it is less than the Salpeter time t_{Edd} on which the spin magnitudes change. One might therefore be concerned that these distributions have not converged to the value they should have at $r_i \sim 1000M$, where the gravitational-wave driven stage of the inspiral begins.

Given the strong dependence of predicted SBH spin magnitudes on the underlying assumptions about gas accretion, in this paper we simply assume $\chi_1 = \chi_2 = \chi$ for $\chi = 0.5, 0.75, \text{ and } 1.0$, and provide predictions for each of these three values.

2. Spin Directions

The residual misalignment of the SBH spins with their orbital angular momentum at r_i has been less thoroughly investigated than the spin magnitudes. The simulations of Dotti et al. [17] began with one $4 \times 10^6 M_\odot$ SBH at rest at the center of a $10^8 M_\odot$ circumnuclear disk. The second SBH, also with $m_i = 4 \times 10^6 M_\odot$, began at an initial separation of $r = 50$ pc with orbital angular momentum that was already aligned or anti-aligned with that of the circumnuclear disk. This is consistent with the SPH simulations of Larwood and Papaloizou [53], which suggest that the mass-quadrupole moment of the SBH binary will induce differential precession in an inclined circumbinary disk. Viscous dissipation will then cause this differentially precessing disk to settle into the equatorial plane of the binary. It is unclear whether this mechanism will operate at the large initial separation of the Dotti et al. simulations before the SBH binary becomes gravitationally bound. Dynamical friction causes initially eccentric or retrograde orbits to circularize as the second SBH inspirals to a final separation $r \simeq 5$ pc. Accretion during this inspiral aligns the spins of both SBHs to within 10° of the orbital angular momentum for a cold circumnuclear disk, and to within 30° for a hot disk with greater pressure support and hence more isotropic gas velocity dispersion [19]. These simulations did not include star

formation or cooling, and the internal energy of the gas particles was chosen to prevent gravitational fragmentation. These choices suppress chaotic accretion and the dynamical instabilities found in Hopkins et al. [51], that cause the direction of the angular momentum of the inner disk to fluctuate on \lesssim Myr timescales. These estimates should therefore be considered lower bounds on the residual misalignment between the SBH spins and their orbital angular momentum.

After the simulations of Dotti et al. [17] end, but before the gravitational-wave driven stage of the inspiral begins at $r_i = 1000M$, the SBHs open a gap and form a true circumbinary disk. High-resolution hydrodynamical simulations indicate that the gas surface density will be sharply truncated at radii less than twice the semi-major axis of the binary [54]. Mass can flow from the inner edge of this circumbinary disk onto the individual SBHs [13, 55]. Accretion rates are generally higher for the less massive SBH, which is further from the center of mass and hence closer to the inner edge of the disk. This point is absolutely crucial for the PN spin alignment that is the subject of this paper, as it is the *relative* value of θ_1 and θ_2 that determines whether gravitational recoils are suppressed or enhanced. One might expect that the higher accretion rate onto the smaller SBH would lead to closer alignment between its spin and that of the orbital angular momentum. Alternatively, it is possible that the spin of the more massive SBH would be more influential in determining the direction of the warp in the circumbinary disk that torques the SBH spins. The relative value of θ_1 and θ_2 in the presence of a circumbinary disk remains very much an open question.

A final complication is the growth of the binary’s orbital eccentricity through its interaction with the circumbinary disk [56]. Although dynamical friction damped the orbital eccentricity at the large separations of the Dotti et al. simulations [17], after the formation of a circumbinary disk the orbital eccentricity again grows to a limiting value $e_{\text{crit}} \simeq 0.7$ [57]. Gravitational radiation circularizes the binary after it decouples from the circumbinary disk [58], but the binary could still have considerable residual eccentricity $e_{\text{LISA}} \propto M^{-0.73} q^{-1.2}$ when the frequency of the fundamental GW harmonic reaches $f_{\text{LISA}} = 10^{-4}$ Hz [57, 59].

We will neglect residual eccentricity during the inspiral and any effects it might have on PN spin alignment. To encompass all possible scenarios with regard to astrophysical spin alignment prior to $r_i = 1000M$, in our simulations we will consider:

- 1) Uniform symmetric distributions in $\cos\theta_1$ and $\cos\theta_2$ drawn in the range $\theta_i \in [0^\circ, 10^\circ]$ ($i = 1, 2$; strong alignment) and $\theta_i \in [0^\circ, 30^\circ]$ (weak alignment). We will refer to these cases as the “10/10” and “30/30” scenarios.
- 2) A uniform distribution in $\cos\theta_1$ and $\cos\theta_2$ with asymmetric range for the angles: $\theta_1 \in [0^\circ, 10^\circ]$, $\theta_2 \in [0^\circ, 30^\circ]$. In this “10/30” scenario the primary

is more strongly aligned with the orbital angular momentum.

- 3) A uniform distribution in $\cos\theta_1$ and $\cos\theta_2$ with $\theta_1 \in [0^\circ, 30^\circ]$, $\theta_2 \in [0^\circ, 10^\circ]$. This “30/10” scenario could result from the secondary orbiting close to the inner edge of a circumbinary disk, so that it ends up being more aligned than the primary with the orbital angular momentum.

IV. RESULTS

We carried out a systematic study of the probability that gravitational recoils eject SBHs from their host galaxies. We generated a population of binaries with astrophysically motivated mass ratios using the Monte Carlo prescription described in Section III A. To quantify the effect of SBH spin magnitudes, we computed ejection probabilities for three fixed values of $\chi_1 = \chi_2 = \chi$: $\chi=0.5, 0.75$, and 1. To account for all possibilities given the great uncertainty in the spin-alignment distributions, we considered the four cases described in Section III B 2: two “symmetric” cases (10/10, 30/30) and two “asymmetric” cases (10/30 and 30/10).

Our results for $\chi = 1$ are summarized in Figure 3. This figure has four panels: our simulated binaries are binned by mass ratio q in the top panels, and by the stellar mass M_* of the larger host galaxy in the bottom panels. In the right panels we assume that a gravitational recoil greater than $v_{\text{ej}} = 1,000$ km/s is needed to eject a recoiling SBH from its host galaxy, while in the left panels we adopt a prescription that depends on the stellar mass M_* . The gravitational potential of a real galaxy is the sum of contributions from its stellar mass and DM halo; although the DM halo is more massive, the more concentrated stellar contribution is dominant for large elliptical galaxies [27]. Modeling elliptical galaxies with the density profiles of Terzić and Graham [60], Gualandris and Merritt [61] find that escape velocities have typical values $v_{\text{esc}} \simeq 2.1(GM_*/R_e)^{1/2}$, where R_e is the effective radius that contains half the galaxy’s total luminosity. Combining this with the observed relation $R_e \approx 1.2 \text{ kpc}(M_*/10^{10}M_\odot)^{0.075}$ yields the approximate expression [61]

$$v_{\text{esc}} \simeq 1,154 \text{ km/s} \left(\frac{M_*}{10^{11}M_\odot} \right)^{0.4625}. \quad (7)$$

This is the prescription we used to calculate escape velocities in the left panels of Figure 3.

Each panel of Figure 3 has 7 histograms: the solid black curve corresponds to the total distribution of simulated binaries, while the 6 dashed and/or dotted colored curves correspond to the distributions of ejected SBHs given the 6 different spin-alignment distributions indicated in the keys to the figure. PN spin alignment can play an important role for asymmetric distributions, as

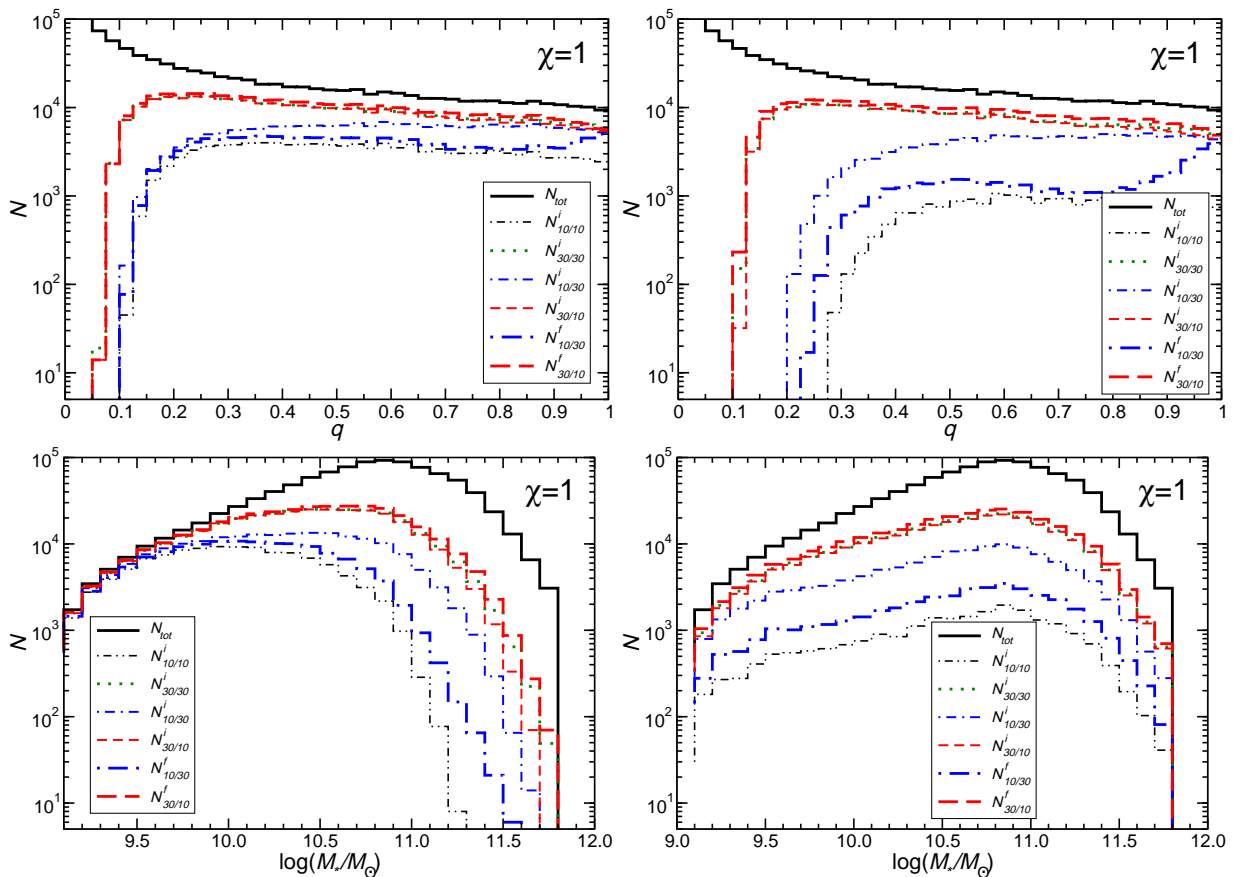


FIG. 3. Distributions of ejected remnants as functions of the binary mass ratio (top) and of the mass of the host galaxy (bottom). Left panels: v_{ej} is computed using Eq. (7). Right: we use a constant ejection velocity $v_{\text{ej}} = 1,000$ km/s. In the asymmetric cases (10/30 and 30/10) thin lines refer to kicks computed using the initial spin distributions, while thick lines refer to kicks computed from the final distributions.

can be seen by comparing the distributions of ejected binaries calculated from spins *before* (thin-line dashed and dash-dotted histograms) or *after* (thick-line histograms) the PN evolution from $r_i = 1000M$ to $r_f = 10M$. As expected, the fraction of ejected binaries decreases in the 10/30 case, while it increases in the 30/10 case. However, the kick reduction in the 10/30 case is more significant than the kick enhancement in the 30/10 case: in other words, *PN resonances are more effective at reducing recoils when the primary is more aligned with the orbital angular momentum than they are at increasing recoils when the secondary is more aligned with the orbital angular momentum*. For the symmetric distributions (10/10 and 30/30), PN spin alignment has a marginal effect on the ejection probabilities¹. For clarity (and to save computational time) we only plot the distribution of ejected binaries that results by applying the recoil formula to

¹ We have checked this statement by running PN evolutions in the 10/10 case. The “initial” and “final” distributions of ejected merger remnants are very similar.

the initial distribution at $r_i = 1000M$ in these symmetric cases.

Comparing the left and right panels of Figure 3 allows us to understand the effects of the mass-dependent escape velocity of Eq. (7) on the ejection probability. The most obvious effect is the steep decrease in the ejected fraction from near unity at $M_* \lesssim 10^{10}M_\odot$ to less than 10% for $M_* \gtrsim 10^{11}M_\odot$. This is very natural: heavier galaxies should be more effective at retaining recoiling SBHs. Somewhat more surprising is that despite the constant escape velocity, the escape fraction also increases as $M_* \rightarrow 10^9M_\odot$ in the bottom right panel. This is a consequence of our decision to neglect SBHs with $m_2 < 10^6M_\odot$ that reside in galaxies with $m_* < 10^9M_\odot$. Because of this choice, SBHs in galaxies with $M_* \simeq 10^9M_\odot$ only undergo comparable-mass ($q \simeq 1$) mergers, elevating the fraction of large recoils since kicks are proportional to $q^2/(1+q)^5$ at leading order (see Eq. (11) of [26]).

A second effect of the mass-dependent escape velocity of Eq. (7) is the possibility of ejecting recoiling SBHs for mass ratios as low as $q \simeq 0.1$, as can be seen in the top left panel of Figure 3. The larger host galaxy can have a mass

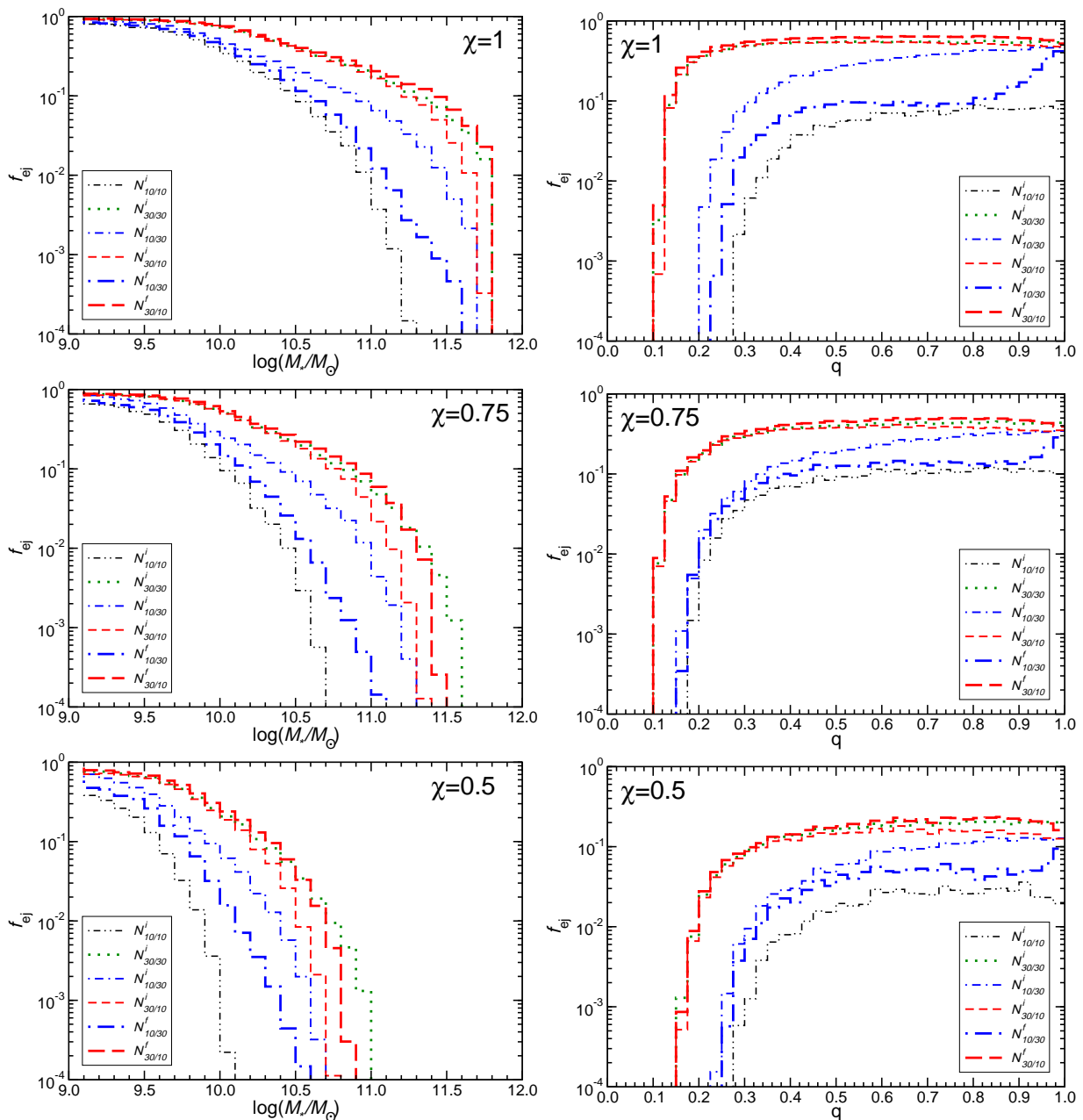


FIG. 4. Fraction f_{ej} of ejected remnants as functions of the mass of the host galaxy (left) and of the binary mass ratio (right). Here v_{ej} is computed using Eq. (7) and we vary the dimensionless spin parameter $\chi = \chi_1 = \chi_2$.

as small as $10^{10}M_{\odot}$ for these mass ratios, corresponding to an escape velocity $v_{\text{esc}} \simeq 400 \text{ km/s} < 1,000 \text{ km/s}$ by Eq. (7). This accounts for the nonzero escape probabilities for $q < 0.1$. We also note that in preparing these figures we have not evolved any PN inspirals for $q < 0.1$, even for those histograms labeled with N^f that correspond to evolved distributions. This explains why the thin and thick lines corresponding to the initial and final histograms coincide for $q < 0.1$. The gravitational-wave inspiral time is inversely proportional to the binary’s symmetric mass ratio $\eta = q/(1+q)^2$ [58], making

it hard to preserve accuracy over long PN time evolutions for $q < 0.1$. However, Schnittman [20] showed that spin-orbit resonances only become important inside a “resonance locking” radius $r_{\text{lock}}/M \approx [(1+q^2)/(1-q^2)]^2$. We are therefore justified in treating all binaries with $q \leq 0.1$ (for which PN evolutions from $r_i = 1000M$ to $r_f = 10M$ become problematic) as if the inspiral did not happen: that is, we can compute recoils of binaries with $q < 0.1$ by simply applying the recoil formula at $r = r_i$.

We examine how the fraction f_{ej} of ejected SBHs depends on the SBH spin magnitude χ in Figure 4. The two

top panels in this figure were produced using the same distributions shown in the left panels of Figure 3; the fraction f_{ej} is calculated by dividing the histograms for each spin distribution by the solid black histogram showing the total distribution. As expected, the ejected fractions are smaller for lower values of χ , since the kick magnitudes are reduced while the escape velocities remain fixed. Ejections from host galaxies with $M_* \gtrsim 10^{11.5} M_\odot$ ($10^{11} M_\odot$) are nearly eliminated for $\chi \lesssim 0.75$ (0.5). PN spin alignment remains effective for these lower spin magnitudes; for certain values of M_* , the ejected fraction is reduced by almost an order of magnitude. Careful scrutiny of the left panels of Figure 4 reveals that PN kick enhancement for the 30/10 case drives f_{ej} above that of the 30/30 case except at the highest values of M_* for the $\chi = 0.5$ and 0.75 distributions. Mergers involving the most massive host galaxies are dominated by small values of q , for which PN spin alignment is ineffective.

It is also interesting to note that PN spin alignment is suppressed as $q \rightarrow 1$ (the thin and thick lines converge in this limit in the right panels of Figure 4). Schnittman [20] showed that PN spin alignment increased as q increased from 1/9 up to 9/11 (see Figure 10 of [20]). Symmetry implies that PN spin alignment must vanish for equal-mass binaries, since the labeling of the SBHs is arbitrary for $q = 1$ and it is therefore impossible to distinguish $\theta_1 < \theta_2$ from $\theta_2 > \theta_1$. This limiting behavior implies that the effects of spin alignment must be maximized for some mass ratio in the range $0.8 \leq q \leq 1$, which is precisely what we observe in the right panels of Figure 4. These near-unity mass ratios are also expected to yield the largest kicks, which emphasizes the importance of including the effects of PN spin alignment in future studies of gravitational recoils.

A final summary of our results is provided in Table I, where we calculate the percentage of ejected binaries for each spin distribution. Although the precise amount of spin alignment depends on the value of χ , we see that kicks are suppressed (enhanced) by $\sim 40\%$ (20%) when the escape velocities are given by Eq. (7). The kick suppression or enhancement is even more dramatic for the case of a constant escape velocity $v_{\text{ej}} = 1,000$ km/s. The ejected fraction is lower overall for this choice of escape velocity, which is larger than the mean value predicted by Eq. (7). The kick suppression or enhancement is greater because the effects of PN spin alignment are most pronounced at the high-velocity tail of the kick distribution, as shown in the left panel of Figure 2.

V. DISCUSSION

We demonstrated in previous work [22] that the alignment of SBH spins with each other during the PN stage of the inspiral can dramatically suppress the predicted distribution of gravitational recoils. This mechanism can

χ	$(10/10)_i$	$(30/30)_i$	$(10/30)_i$	$(10/30)_f$	$(30/10)_i$	$(30/10)_f$
v_{ej} given by Eq. (7)						
0.50	0.76	7.21	2.95	1.59	6.03	7.81
0.75	3.86	19.28	9.208	5.310	17.79	21.41
1.00	11.22	34.26	19.49	13.70	33.60	37.11
$v_{\text{ej}} = 1,000$ km/s						
0.50	0	0.39	0	0	0	0.002
0.75	0	10.30	2.21	0.13	7.70	12.92
1.00	2.21	27.57	12.18	4.19	26.87	31.22

TABLE I. Percentage of ejected binaries for different values of the spin and different combinations of the angles (θ_1, θ_2). A column header such as “(10/30) $_i$ ” means that the probability was computed considering the spin distribution before PN evolutions, while “(10/30) $_f$ ” means that the probability was computed applying the recoil formula at the end of the PN evolution. In the top rows we assume that the escape velocity v_{ej} is given by Eq. (7); in the bottom rows we assume a constant $v_{\text{ej}} = 1,000$ km/s.

reinforce the kick suppression that results from the alignment of the SBH spins with their orbital angular momentum through interaction with a circumbinary disk at an earlier stage of the inspiral [16]. Recent NR simulations [25, 26] showed that gravitational recoils are maximized not in the previously claimed “superkick” configuration in which the spins lie in the orbital plane, but in a new “hang-up” configuration in which the angle between the spins and orbital angular momentum is $\sim 50^\circ$. The primary conclusion of this paper is that kick suppression due to PN spin alignment remains highly effective despite the new dependence of the gravitational recoil on SBH spins.

It is difficult to make very robust quantitative predictions about the magnitude of this effect, as the recoil distribution is highly sensitive to SBH spin distributions that are theoretically uncertain and poorly constrained observationally. Some SPH simulations have shown that SBH spins can grow to large magnitudes and rapidly align with the orbital angular momentum through coherent accretion from a massive circumnuclear disk [19], but other simulations that include gas cooling and star formation indicate that the direction of the angular momentum of the accreted gas will vary chaotically on timescales comparable to the alignment time, leading to smaller spin magnitudes and larger misalignments with the orbital angular momentum [51]. Our results show that the predicted fraction of recoiling SBHs that are ejected from their host galaxies can vary from $\lesssim 10^{-2}$ to $\sim 1/3$ depending on the adopted distribution of SBH spins. Although somewhat frustrating from a theoretical perspective, the strong dependence of the ejected fraction on SBH spins implies that observational studies of recoils may place promising constraints on the highly elusive SBH spin distribution.

Our work in this paper reveals several of the issues that must be addressed before we can predict recoil distribu-

tions with confidence:

- 1) We need to determine how effectively realistic circumbinary disks can align SBH spins with their orbital angular momentum. Such circumbinary disks may not remain geometrically thin, and may gravitationally fragment or collapse into stars. These possibilities could have significant quantitative effects on the SBH spin distribution at the onset of the PN stage of the inspiral.
- 2) We need to develop a better understanding of the interaction between unequal-mass SBHs and a circumbinary disk. One could argue that the spin of either the primary or the secondary might align more efficiently with the orbital angular momentum. Whether PN spin alignment leads to kick suppression or enhancement depends crucially on the *relative* values of θ_1 and θ_2 .
- 3) We need to carefully consider how the merger rate, mass-ratio distribution, and escape velocity depend on host-galaxy mass. Our results shown in Figs. 3 and 4 demonstrate the sensitivity of the ejected

fraction to assumptions about these galactic properties.

Although challenging, steady theoretical and observational progress is being made on all of these issues. Once astrophysicists can provide more accurate predictions of SBH spin distributions at $r_i \sim 1000M$, when SBHs decouple from their circumbinary disks, relativists will be able to evolve the binaries through merger and more accurately predict gravitational recoils. Including the PN stage of the inspiral will be an important ingredient in this grand theoretical undertaking.

Acknowledgements. We thank Massimo Dotti, Mike Eracleous, Carlos Lousto, David Merritt, Jeremy Tinker, Marta Volonteri, and Yosef Zlochower for useful conversations. This work was supported by NSF Grants PHY-090003, PHY-0900735 and PHY-1055103, FCT projects PTDC/FIS/098032/2008 and PTDC/FIS/098025/2008, the Ramón y Cajal Programme and Grant FIS2011-30145-C03-03 of the Ministry of Education and Science of Spain, the FP7-PEOPLE-2011-CIG Grant CBHEO, No. 293412, the Sherman Fairchild Foundation to Caltech, projects ICTS-CESGA-221 of the Centro de Supercomputación de Galicia, AECT-2011-3-0007 by the Barcelona Supercomputing Center, and the ERC Starting Grant ERC-2010-Stg-DyBHo.

-
- [1] J. Kormendy and D. Richstone, *ARA&A* **33**, 581 (1995).
 - [2] J. Magorrian *et al.*, *Astron. J* **115**, 2285 (1998), [astro-ph/9708072](#).
 - [3] K. Gebhardt, R. Bender, G. Bower, A. Dressler, S. M. Faber, A. V. Filippenko, R. Green, C. Grillmair, L. C. Ho, J. Kormendy, T. R. Lauer, J. Magorrian, J. Pinkney, and S. Richstone, *D. Tremaine*, *Astrophys. J* **539**, L13 (2000), [astro-ph/0006289](#).
 - [4] M. J. Fitchett, *Mon. Not. R. Astron. Soc.* **203**, 1049 (1983).
 - [5] M. Favata, S. A. Hughes, and D. E. Holz, *Astrophys. J* **607**, L5 (2004), [astro-ph/0408492](#).
 - [6] F. Pretorius, *Phys. Rev. Lett.* **95**, 121101 (2005), [gr-qc/0507014](#).
 - [7] M. Campanelli, C. O. Lousto, P. Marronetti, and Y. Zlochower, *Phys. Rev. Lett.* **96**, 111101 (2006), [gr-qc/0511048](#).
 - [8] J. G. Baker, J. Centrella, D.-I. Choi, M. Koppitz, and J. van Meter, *Phys. Rev. Lett.* **96**, 111102 (2006), [gr-qc/0511103](#).
 - [9] J. A. González, U. Sperhake, B. Brügmann, M. D. Hannam, and S. Husa, *Phys. Rev. Lett.* **98**, 091101 (2007), [gr-qc/0610154](#).
 - [10] J. A. González, M. D. Hannam, U. Sperhake, B. Brügmann, and S. Husa, *Phys. Rev. Lett.* **98**, 231101 (2007), [gr-qc/0702052](#).
 - [11] M. Campanelli, C. O. Lousto, Y. Zlochower, and D. Merritt, *Astrophys. J.* **659**, L5 (2007).
 - [12] M. C. Begelman, R. D. Blandford, and M. J. Rees, *Nature* **287**, 307 (1980).
 - [13] P. Artymowicz and S. H. Lubow, *Astrophys. J.* **467**, L77 (1996).
 - [14] J. M. Bardeen and J. A. Petterson, *Astrophys. J.* **195**, L65 (1975).
 - [15] A. Perego, M. Dotti, M. Colpi, and M. Volonteri, *Mon. Not. R. Astron. Soc.* **399**, 2249 (2009), [arXiv:0907.3742 \[astro-ph.CO\]](#).
 - [16] T. Bogdanović, C. S. Reynolds, and M. C. Miller, *Astrophys. J.* **661**, L147 (2007).
 - [17] M. Dotti, M. Ruzzkowski, L. Paredi, M. Colpi, M. Volonteri, and F. Haardt, *Mon. Not. R. Astron. Soc.* **396**, 1640 (2009), [arXiv:0902.1525 \[astro-ph.CO\]](#).
 - [18] H. Bondi and F. Hoyle, *Mon. Not. R. Astron. Soc.* **104**, 273 (1944).
 - [19] M. Dotti, M. Volonteri, A. Perego, M. Colpi, M. Ruzzkowski, and F. Haardt, *Mon. Not. R. Astron. Soc.* **402**, 682 (2010), [arXiv:0910.5729 \[astro-ph.HE\]](#).
 - [20] J. D. Schnittman, *Phys. Rev. D* **70**, 124020 (2004).
 - [21] M. Kesden, U. Sperhake, and E. Berti, *Phys. Rev. D* **81**, 084054 (2010).
 - [22] M. Kesden, U. Sperhake, and E. Berti, *Astrophys. J.* **715**, 1006 (2010).
 - [23] L. Boyle, M. Kesden, and S. Nissanke, *Phys. Rev. Lett.* **100**, 151101 (2008), [arXiv:0709.0299 \[gr-qc\]](#).
 - [24] L. Boyle and M. Kesden, *Phys. Rev. D* **78**, 024017 (2008), [arXiv:0712.2819 \[astro-ph\]](#).
 - [25] C. O. Lousto and Y. Zlochower, *Phys. Rev. Lett.* **107**, 231102 (2011), [arXiv:1108.2009 \[gr-qc\]](#).
 - [26] C. O. Lousto, Y. Zlochower, M. Dotti, and M. Volonteri, *ArXiv e-prints* (2012), [arXiv:1201.1923 \[gr-qc\]](#).

- [27] D. Merritt, M. Milosavljević, M. Favata, S. Hughes, and D. Holz, *Astrophys. J.* **607**, L9 (2004).
- [28] D. Lynden-Bell, *Nature* **223**, 690 (1969).
- [29] M. G. Haehnelt and M. J. Rees, *Mon. Not. R. Astron. Soc.* **263**, 168 (1993).
- [30] W. H. Press and P. Schechter, *Astrophys. J.* **187**, 425 (1974).
- [31] G. Lodato and P. Natarajan, *Mon. Not. R. Astron. Soc.* **371**, 1813 (2006), arXiv:astro-ph/0606159.
- [32] V. Bromm, P. S. Coppi, and R. B. Larson, *Astrophys. J.* **527**, L5 (1999), arXiv:astro-ph/9910224.
- [33] M. Volonteri, F. Haardt, and P. Madau, *Astrophys. J.* **582**, 559 (2003), astro-ph/0207276.
- [34] J. E. Plowman, R. W. Hellings, and S. Tsuruta, *Mon. Not. R. Astron. Soc.* **415**, 333 (2011), arXiv:1009.0765 [astro-ph.CO].
- [35] J. R. Gair, A. Sesana, E. Berti, and M. Volonteri, *Class.Quant.Grav.* **28**, 094018 (2011), arXiv:1009.6172 [gr-qc].
- [36] A. Sesana, J. Gair, E. Berti, and M. Volonteri, *Phys.Rev.* **D83**, 044036 (2011), arXiv:1011.5893 [astro-ph.CO].
- [37] P. Amaro-Seoane, S. Aoudia, S. Babak, P. Binétruy, E. Berti, A. Bohé, C. Caprini, M. Colpi, N. J. Cornish, K. Danzmann, J.-F. Dufaux, J. Gair, O. Jennrich, P. Jetzer, A. Klein, R. N. Lang, A. Lobo, T. Littenberg, S. T. McWilliams, G. Nelemans, A. Petiteau, E. K. Porter, B. F. Schutz, A. Sesana, R. Stebbins, T. Sumner, M. Vallisneri, S. Vitale, M. Volonteri, and H. Ward, *ArXiv e-prints* (2012), arXiv:1201.3621 [astro-ph.CO].
- [38] K. R. Stewart, J. S. Bullock, E. J. Barton, and R. H. Wechsler, *Astrophys.J.* **702**, 1005 (2009), arXiv:0811.1218 [astro-ph].
- [39] D. Merritt and L. Ferrarese, *Mon. Not. R. Astron. Soc.* **320**, L30 (2001), astro-ph/0009076.
- [40] A. Leauthaud, J. Tinker, K. Bundy, P. S. Behroozi, R. Massey, *et al.*, *Astrophys. J.* **744**, 159 (2012), arXiv:1104.0928 [astro-ph.CO].
- [41] B. Panter, R. Jimenez, A. F. Heavens, and S. Charlot, *Mon. Not. R. Astron. Soc.* **378**, 1550 (2007), arXiv:astro-ph/0608531.
- [42] I. K. Baldry, K. Glazebrook, and S. P. Driver, *Mon. Not. R. Astron. Soc.* **388**, 945 (2008), arXiv:0804.2892.
- [43] C. Li and S. D. M. White, *Mon. Not. R. Astron. Soc.* **398**, 2177 (2009), arXiv:0901.0706 [astro-ph.CO].
- [44] M. Volonteri, P. Madau, E. Quataert, and M. Rees, *Astrophys. J.* **620**, 69 (2005), astro-ph/0410342.
- [45] N. I. Shakura and R. A. Sunyaev, *Astron. Astrophys.* **24**, 337 (1973).
- [46] K. S. Thorne, *Astrophys. J.* **191**, 507 (1974).
- [47] C. F. Gammie, S. L. Shapiro, and J. C. McKinney, *Astrophys. J.* **602**, 312 (2004), arXiv:astro-ph/0310886.
- [48] R. Moderski and M. Sikora, *Astron. Astrophys. Suppl. Ser.* **120**, 591 (1996).
- [49] A. S. Wilson and E. J. M. Colbert, *Astrophys. J.* **438**, 62 (1995), arXiv:astro-ph/9408005.
- [50] A. R. King, J. E. Pringle, and J. A. Hofmann, *Mon. Not. R. Astron. Soc.* **385**, 1621 (2008), arXiv:0801.1564 [astro-ph].
- [51] P. F. Hopkins, L. Hernquist, C. C. Hayward, and D. Narayanan, *ArXiv e-prints* (2011), arXiv:1111.1236 [astro-ph.CO].
- [52] E. Berti and M. Volonteri, *Astrophys. J.* **684**, 822 (2008), arXiv:0802.0025 [astro-ph].
- [53] J. D. Larwood and J. C. B. Papaloizou, *Mon. Not. R. Astron. Soc.* **285**, 288 (1997), arXiv:astro-ph/9609145.
- [54] A. I. MacFadyen and M. Milosavljević, *Astrophys. J.* **672**, 83 (2008), arXiv:astro-ph/0607467.
- [55] K. Hayasaki, S. Mineshige, and H. Sudou, *Publications of the Astronomical Society of Japan* **59**, 427 (2007), arXiv:astro-ph/0609144.
- [56] J. C. B. Papaloizou, R. P. Nelson, and F. Masset, *Astron. Astrophys.* **366**, 263 (2001).
- [57] C. Roedig, M. Dotti, A. Sesana, J. Cuadra, and M. Colpi, *Mon. Not. R. Astron. Soc.* **415**, 3033 (2011), arXiv:1104.3868 [astro-ph.CO].
- [58] P. C. Peters, *Phys. Rev.* **136**, B1224 (1964).
- [59] N. Yunes, K. Arun, E. Berti, and C. M. Will, *Phys.Rev.* **D80**, 084001 (2009), arXiv:0906.0313 [gr-qc].
- [60] B. Terzic and A. W. Graham, *Mon. Not. R. Astron. Soc.* **362**, 197 (2006), arXiv:astro-ph/0506192 [astro-ph].
- [61] A. Gualandris and D. Merritt, *Astrophys. J.* **678**, 780 (2008), arXiv:0708.0771 [astro-ph].